III International Conference on Particle-based Methods – Fundamentals and Applications
PARTICLES 2013
M. Bischoff, E. Oñate, D.R.J. Owen, E. Ramm & P. Wriggers (Eds)

NUMERICAL SIMULATION OF A SMALL SCALE DYNAMIC REPLACEMENT STONE COLUMN CREATION EXPERIMENT

WOJCIECH T. SOŁOWSKI [*], SCOTT W. SLOAN[2], PIOTR T. KANTY[3] AND SŁAWOMIR KWIECIEŃ[4]

[*] ARC Centre of Excellence for Geotechnical Science and Engineering
Faculty of Engineering and Built Environment
University of Newcastle
2291 Callaghan, NSW, Australia
wojciech.solowski@newcastle.edu.au
http://www.newcastle.edu.au/research-centre/cgmm/publications/wojciech-solowski.html

[2] ARC Centre of Excellence for Geotechnical Science and Engineering
Faculty of Engineering and Built Environment
University of Newcastle
2291 Callaghan, NSW, Australia
scott.sloan@newcastle.edu.au
http://www.newcastle.edu.au/research-centre/cgmm/publications/scott-sloan.html

[3] Katedra Geotechniki
Faculty of Civil Engineering
Silesian University of Technology,
ul. Akademicka 5, Gliwice, Poland
piotr.kanty@polsl.pl

[4] Katedra Geotechniki
Faculty of Civil Engineering
Silesian University of Technology,
ul. Akademicka 5, Gliwice, Poland
slawomir.kwiecien@polsl.pl

Key words: Material Point Method, Dynamic soil exchange, Constitutive modelling
Abstract. The creation of dynamic replacement stone columns is a poorly understood process that is difficult to model numerically due to very large displacements and the complex interactions between the soil and the forming stone column. In this paper the authors use the material point method to approximate a well-documented experiment of the creation of a small scale dynamic replacement soil column. In this experiment the column has been formed in a transparent container (66x60x12 cm) filled with sawdust. The material point simulation aims to replicate the dynamic replacement experiment using basic constitutive models. The computational results are compared with those obtained in the experiment.

1 INTRODUCTION

The dynamic replacement technique is used to reinforce weak soils (especially soils which can be significantly compressed, e.g. soils with organic content or weak clay soils). The soil is reinforced by initially dropping a large weight (typically 10-12 t) from a significant height (10-25m). The resulting crater is filled with a stronger material (gravel or similar), and the weight is dropped again. The new crater is again filled with the stronger material and the procedure continues, usually to the point where the dropped weight does not penetrate the soil any further. The procedure results in a column of a stronger material, which can sustain much higher loads than the soil in its initial condition.

Also the ground surrounding the column is strengthened, as the created gravel column acts as a drain to the original, now somewhat compressed, soil and aids its consolidation.

The dynamic replacement procedure is notoriously difficult to model numerically due to the very large deformation and the complex soil behaviour that takes place. This paper performs a numerical analysis, using the material point method, of a small-scale laboratory experiment where a column is formed in sawdust.

2 SHORT OVERWIEW OF MATERIAL POINT METHOD

The material point method is a numerical method originating from the FLIP method [1] and was originally developed by Sulsky et al. [2]. The explicit version of the method has been further improved, see references [3-6] among others. In the paper by Bardenhagen & Kober [7] the GIMP version of the method has been introduced. This variant of the material point method has been chosen for the calculations in this paper, as it is the most popular implementation. It is also more numerically efficient than the advanced implementations of material point method, like those proposed by Ma et al. [8] and the Convected Particle Domain Interpolation (CPDI) [9, 10]. With those latter, some stability problems are sometimes encountered which can become serious for complicated cases. It is, however likely that the more advanced material point method interpolations would lead to better accuracy of the results.

During computations with the material point method, the problem is discretised with material points. These points carry all the material properties and information required for the analysis. The material points are cast on a grid. In each time step, the movement of the points is explicitly solved using grid nodes. As the material points interact over the grid nodes, points which do not contribute to the same grid node cannot interact. In particular, in GIMP, a material point of a given material which has been moved too far from its neighbours will stop interacting with them, destroying the continuity of the material. That situation is referred to as material separation. Also, as material separation depends on the grid density, it means that when material separation occurs, the GIMP results become grid dependent. The aim of the more advanced methods like [8-10] is to reduce this grid dependency and not allow for material separation.

In GIMP, the material points have finite constant domains associated with them. Thus, they interact when their domains are, at least partially, in neighbouring (or the same) grid cells. Initially the interaction between the particles is weak, but the bigger the part of the domain that is in the neighbouring (or same) grid cell, the stronger the interaction. Because of the fact that the material points start interacting relatively far from each other, the boundary of the

problem is sometimes not very precisely defined. Additionally, when the forces are very weak, as in the case of light material falling under gravity on to some other stronger material, the interaction starts early and the material points may be in equilibrium at locations which are relatively far from each other. In such a case the material points which separated from the bulk of the material, and subsequently get in contact, may create space which is less dense than the initial material.

3 EXPERIMENT DESCRIPTION

The numerical analysis aims to replicate results of a small-scale laboratory experiment. In the experiment the column was created in a transparent 60x66x12cm box. Initially, the box was filled with sawdust up to a depth of 53 cm. Subsequently, the sawdust was compacted with pressure of approximately 1.7 kPa. After the compaction, a 7-stage experiment commenced. In each stage the soil was impacted by a rammer (once or multiple times). The rammer had barrel-like shape with the bottom and top diameter being 9cm, and the central diameter being 10.5cm. Its height was 20cm and it weighted approximately 10.1 kg.

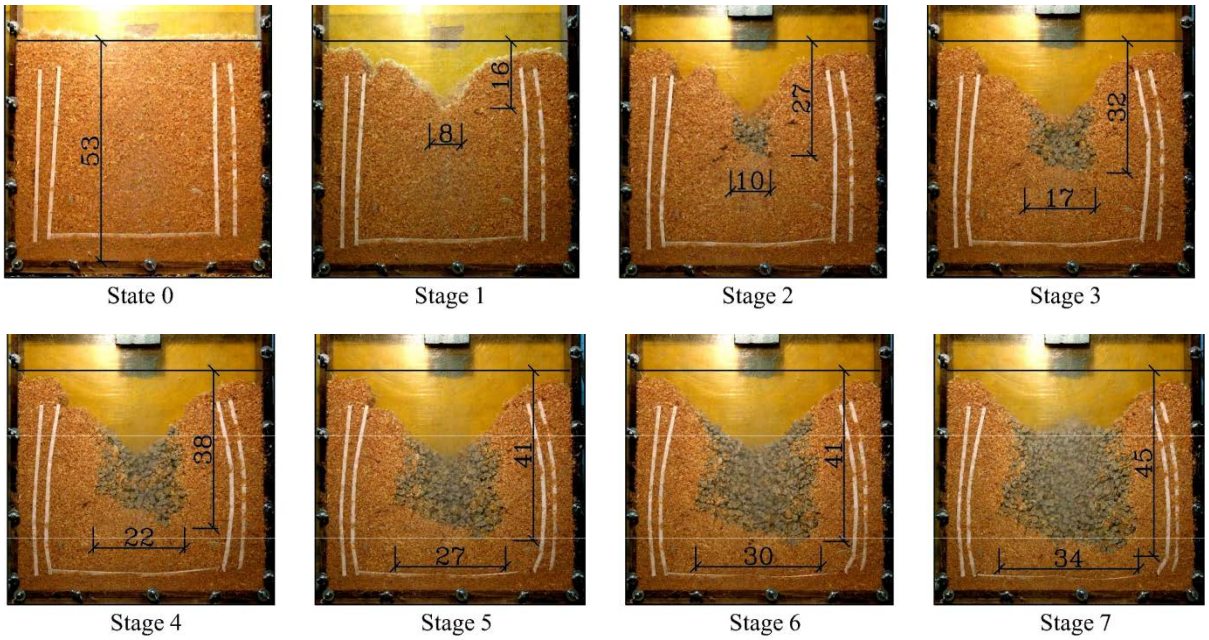

Figure 1: Snapshots of one of the column during formation

During the first stage of the experiment the self-weight of the rammer was used to create the crater. In stage two, the crater was filled with granite gravel and the rammer was dropped from 10 cm height. Each subsequent stage of the experiment was commenced with filling the created crater with granular material. Afterwards, the rammer was dropped from:

- 3 x 10 cm height (stage 3)
- 1 x 10 cm and 3 x 30 cm (stage 4)
- 1 x 30 cm, 1 x 50 cm and 2 x 1m (stage 5)
- 2 x 1m and 1x 1.2 m (stage 6)
- 4 x 1.2 m (stage 7, end of test)

A detailed description of the experiment may be found in Kanty & Sękowski [11]. The column shape and dimensions at each stage of the experiment is given in Fig 1, whereas Figure 2 shows how variable the experimental results were.

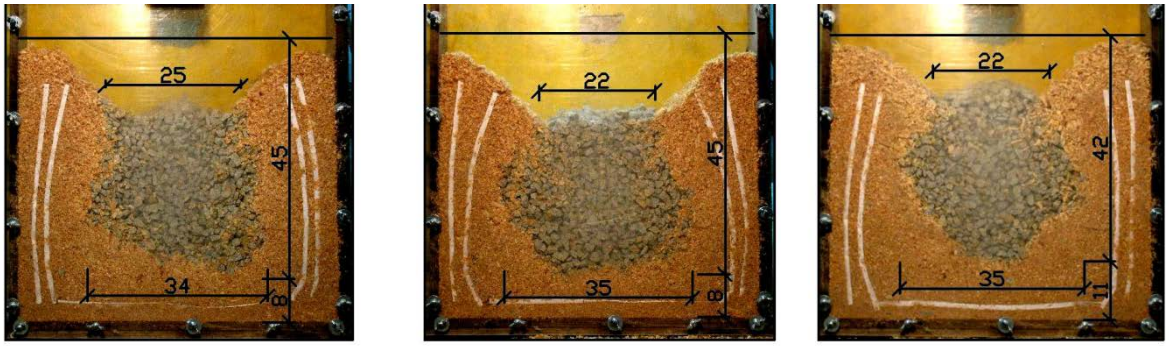

Figure 2: Snapshots and final dimensions of created columns

4 CONSTITUTIVE MODELS USED

The Mohr-Coulomb model has been used to simulate the granite gravel which created the column. This model has been implemented as described in Clausen et al. [12, 13], to ensure that the stress integration is done accurately.
The sawdust has been modelled with an amended Barcelona Basic Model [14], implemented as in [15]. The model was used with the suction equal to zero, as such it is only different to the Modified Cam Clay model because of the non-associated flow rule. However, due to the extreme deformations that occur in the analysis, the Barcelona Basic Model had to be modified to ensure greater stability of the simulation.

4.1 Modifications to the Barcelona Basic Model

The Barcelona Basic Model [14] assumes a constant shear modulus G_0 and a pressure dependent bulk modulus K. This caused instabilities when extreme deformations were encountered, as the G_0 and K values could lead to physically impossible Poisson's ratios. Therefore, the shear modulus is assumed to start to vary at bulk modulus values corresponding to Poisson's ratio of 0.01 and 0.49. Before stress integration, the tangent bulk modulus K is computed as:

$$K = p \cdot (e+1)/\kappa \tag{1}$$

where e is the void ratio, p denotes mean stress and κ is a model parameter. This tangent bulk modulus is used to compute the Poisson's ratio:

$$\nu = \frac{3K - 2G_0}{2(3K + G_0)} \tag{2}$$

If the computed Poisson ratio is outside the range of (0.01, 0.49), it is set to the nearest allowed value (i.e. 0.01 or 0.49) and the shear modulus in the current time step for a given material point is computed as:

$$G = \begin{cases} \dfrac{3K(1-2\cdot 0.01)}{2(1+0.01)} \ \ and \ \ \nu = 0.01 \\ G_0 \ \ when \ \ 0.01 < \nu < 0.49 \\ \dfrac{3K(1-2\cdot 0.49)}{2(1+0.49)} \ \ and \ \ \nu = 0.49 \end{cases} \tag{3}$$

Therefore, when the computed Poisson's ratio is within the allowed range, the shear modulus used is the same as the initial shear modulus G_0.

Also, the critical state soil models require that the mean stress is strictly compressive. That is because of the logarithmic function that is used to compute the elastic void ratio change of the material:

$$\Delta e_{ek} = \kappa \ln \frac{p + \Delta p}{p} \tag{4}$$

Unfortunately, in the Material Point Method, at extreme deformation, material separation can occur and the material points may start to 'float' in space. In these cases, the mean stress may become very low (which slows down the stress integration greatly) or even equal zero. Therefore, an additional yield surface was defined. The elliptic surface is cut-off by a straight plane at very low mean stress p_{min}. The soil behaviour on this yield locus is ideally plastic. That means the mean net stress cannot decrease below p_{min} no matter how deformed the soil is.

5 SIMULATIONS

The material point method calculations were performed using a modified Uintah code, an open source code developed at the University of Utah. The aim of the simulations was to reproduce the laboratory results.

It proved surprisingly difficult to model all the seven stages of the experiment. Although the initial stages could be modelled relatively easily and accurately, a number of stability problems occurred during the later stages. To improve the stability, the changes in the constitutive models described above were necessary. Also, it was difficult to model satisfactorily both the initial and final stages of the experiment using the same set of material parameters.

The problem has been modelled assuming plain strain conditions. To simplify the problem further, it was decided to mode the experiment using symmetry – even though the actual experimental results are to some degree asymmetric.

The grid with the initial arrangement of points is shown in Fig. 3. The granite material used for filling is modelled with four material points per grid cell, whereas the sawdust is modelled with just a single material point per grid cell. To capture the complex shape of the rammer, 4 material points per grid cell were used.

The analysis requires the crater created by the rammer to be filled by the granite granular material. That has been achieved by moving the material points from a "storage" area into the crater in quantities that are required by the crater size. Therefore, a certain amount of space has been used for storing the granular fill material. Similarly, the rammer, during filling is moved into a storage area (as depicted in Fig. 3), and moved back after filling is concluded

and material settled.

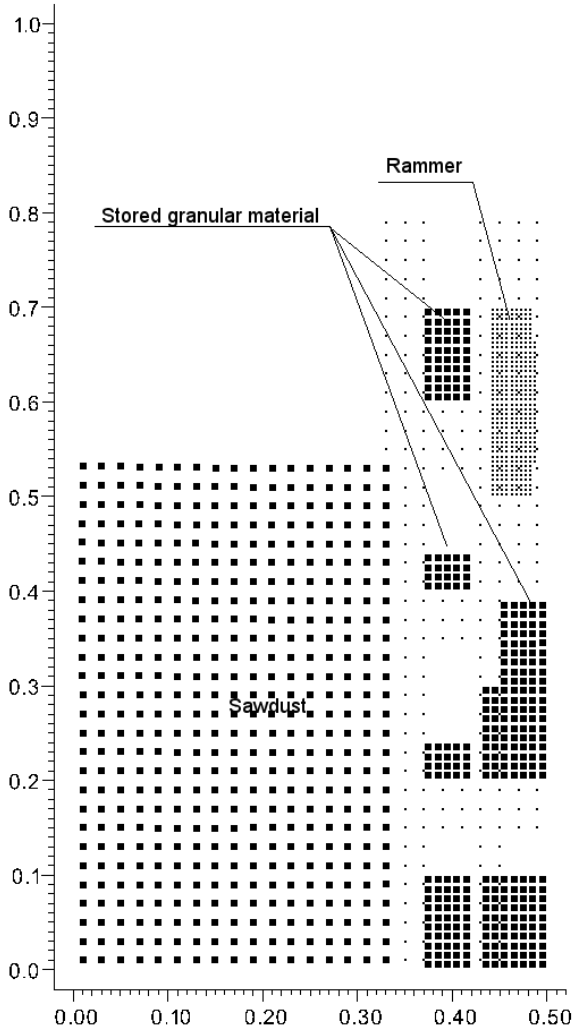

Figure 3: Grid and initial material points positions.

The sawdust material was modelled with the amended Modified Cam Clay model, whereas the granite fill material was modelled with the Mohr-Coulomb model. This was motivated by the granite being relatively incompressible, whereas for the sawdust it was essential to model its compressibility under load.

Choosing material parameters for such an analysis is always a difficult task. Some laboratory tests were made for both materials, though those were better suited for determining the Mohr-Coulomb model parameters. During shear box testing, the friction angle for the granite gravel fill (grain size 5-30 mm) was determined to be 47 degrees. Also, due to grain interlocking, the tests showed some cohesion (up to 20 kPa). The dilation angle was chosen as being 35 degrees lower than the friction angle. The elastic parameters were difficult to assess as they vary depending on the pressure; the values used are given in Table 1.

In the paper two analyses are shown – with higher and a lower cohesion values. Some

cohesion was needed primarily to reduce the number of material points being airborne after the impact of the rammer (the impact of lowering the cohesion is obvious in later parts of the experiment).

Table 1: Material parameters for granite gravel (Mohr – Coulomb model)

Shear modulus [kPa]	Bulk modulus [kPa]	Cohesion [kPa]	Friction angle [deg]	Dilation angle [deg]
240	400	1 8	47	12

The sawdust had friction angle of 37 degrees, which corresponds to a critical state line slope of M=1.51. The elastic parameters were chosen to be a magnitude lower than those of the gravel. Other parameters were chosen to approximate the behaviour of the material observed in the analysis (see Table 2).
To illustrate the impact of the slope of the Normal Compression Line, two parameters were chosen. The higher slope (0.42) was used alongside a lower cohesion value (1 kPa). The impact of this choice is again evident in the later stages of simulation.

Table 2: Material parameters for sawdust (Modified Cam Clay model)

Shear modulus [kPa]	Slope of the elastic loadin-unloading line (κ)	Slope of the Normal Compression Line (λ)	Slope of Critical State Line (M)	Reference pressure [kPa]	Specific volume at reference pressure	Initial hardening parameter value [kPa]	Cut-off pressure (p_{min}) [Pa]
40	0.01	0.42 0.35	1.51	1	2.0	1.7	1E-5

The simulation was performed with the GIMP variant of the material point method. As such, the material points may separate and in those cases some grid-dependency is expected. The frictional contact between the materials is modelled as in [4]. Due to the high friction angles of both the sawdust and the gravel, the friction coefficient was set to 1.

The results of the experiment are given in Figures 4-7. In these figures the arrangement of material points corresponding to sawdust (black) and granite gravel (white) at the end of each stage of the experiment are overlapped over the experimental results. In each figure, the analyses made with alternate sets of model parameters are shown side by side so the impact of the cohesion and the normal compression line slope can be more easily seen.

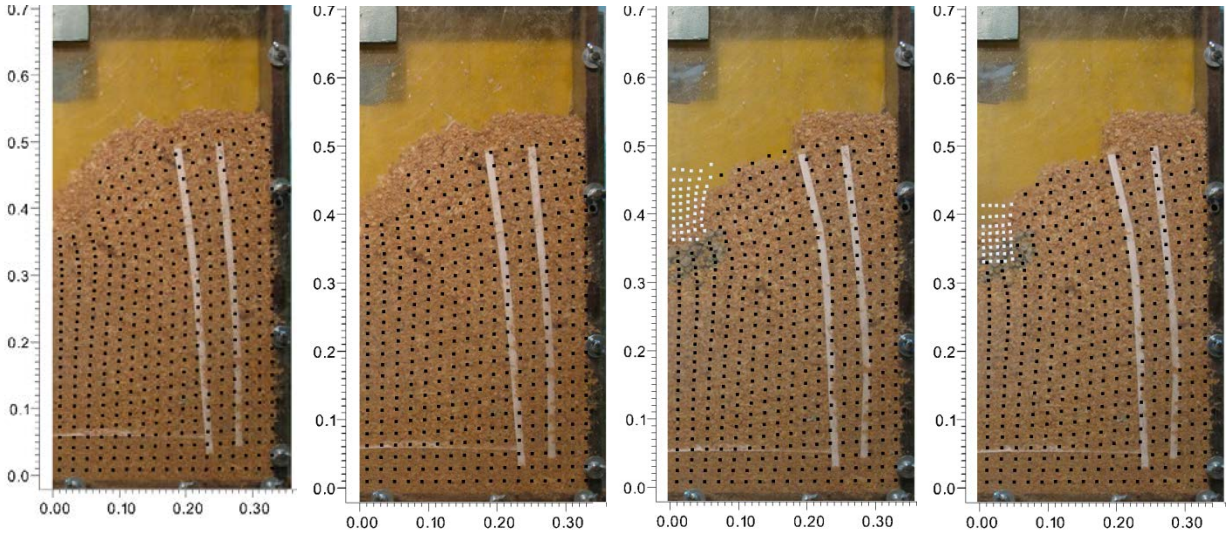

(a) (b)

Figure 4: Comparison of the simulated results with experimental stages 1(left, a) and 2 (right, b). The picture to the left corresponds to more compressible sawdust and the gravel fill with lower cohesion.

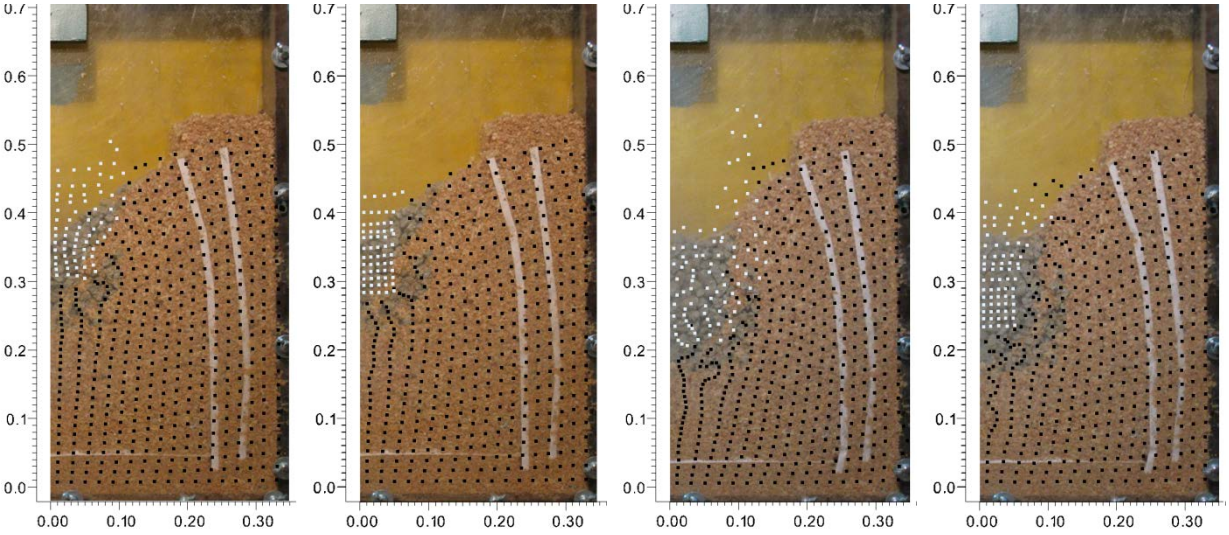

(a) (b)

Figure 5: Comparison of the simulated results with experimental stages 3(left, a) and 4 (right, b). The picture to the left corresponds to more compressible sawdust and gravel fill with lower cohesion.

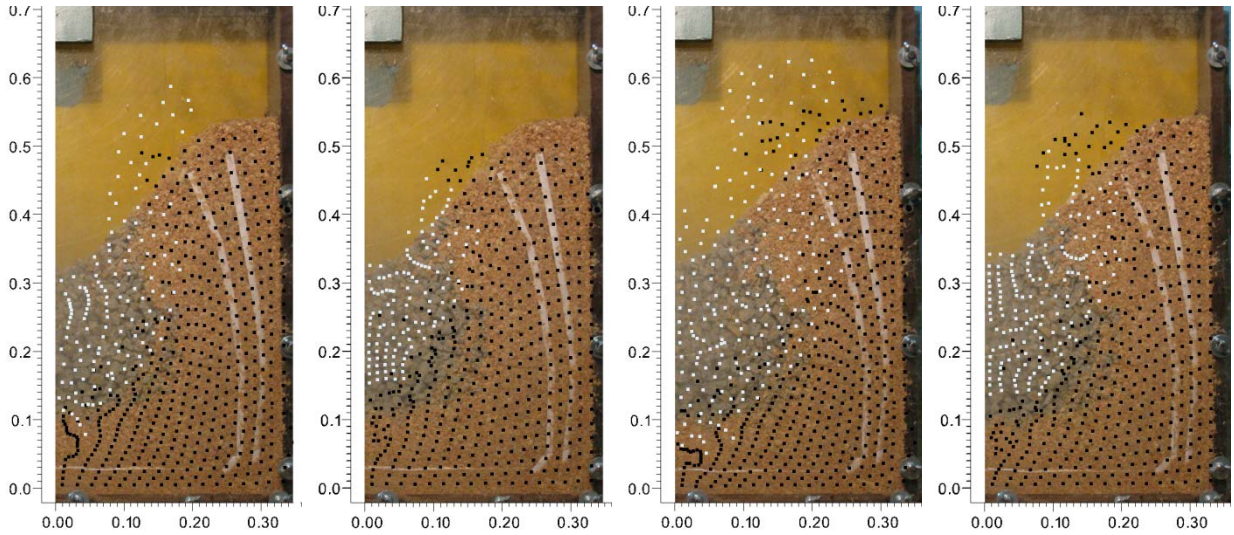

(a) (b)

Figure 6: Comparison of the simulated results with experimental stages 5(left, a) and 6 (right, b). The picture to the left corresponds to more compressible sawdust and the gravel fill with lower cohesion.

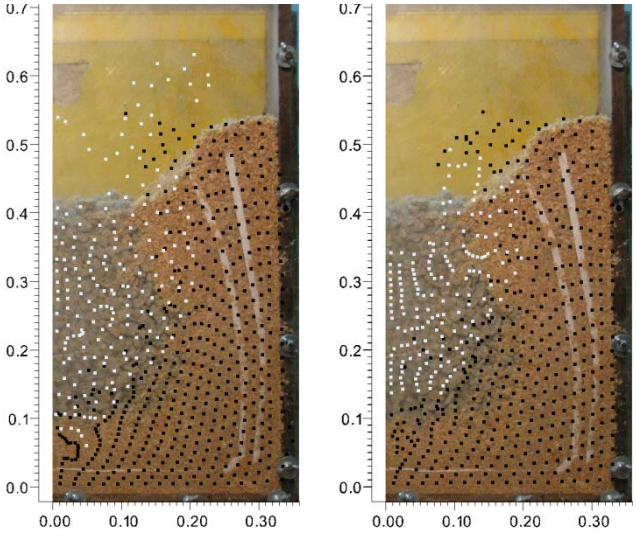

Figure 7: Comparison of the simulated results with final experimental results. The picture to the left corresponds to more compressible sawdust and the gravel fill with lower cohesion.

6 RESULTS ANALYSIS

It may seem at first glance that the results on the right hand side in Figs 4-7, corresponding to the case with the higher cohesion and lower compressibility of the sawdust, predict the results more accurately. Certainly, in the final stages of the experiment, the higher cohesion and lower compressibility resulted in less material separation - thus the 'cloud' of points above the initial level of material is much smaller. Also, the shape of the predicted surface is more accurate. On the other hand, this set of materials resulted in a column which is shorter and narrower at the bottom than the experiment. Also, assuming a relatively high cohesion in

a cohesionless material may be hard to justify.

On the other hand, lowering the cohesion of the gravel fill to a more realistic value, and increasing the compressibility of sawdust, results in an unrealistic shape of the surface in the final stage of the experiment (results on the left hand side of Figs 4-7). However, the column penetration is quite realistic, not only in the final stage, but also in all the later stages. Also, the number of separated points of the fill material may be still acceptable throughout most of the analysis.

Both analyses predict a somewhat wider upper part of the column in the stages 6 and 7. This effect may be due to deficiencies in the constitutive models which, for example, do not take into account rate effects.

The results obtained are quite sensitive to the amount of fill material moved into the crater at the beginning of each stage. In stages 6 & 7, this amount was lowered (in previous stages, the granular material was filling the crater to approximately height of the sawdust, i.e. 53 cm). Should the amount of fill not be lowered, the resulting columns are much wider in the upper part (see Fig 7). The results for the more compressive sawdust and less cohesive fill would replicate the experimental data better if the amount of fill was lowered further in the latter stages of the simulation (stage 3 onwards).

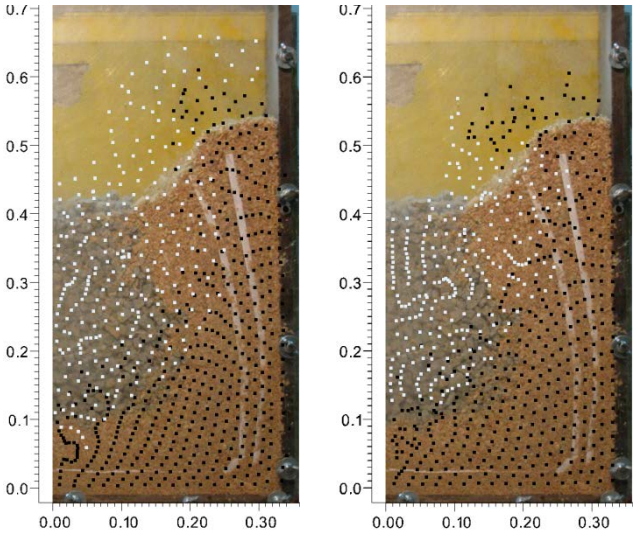

Figure 8: Comparison of the simulated results with the final experimental results. The picture to the left corresponds to more compressible sawdust and gravel with lower cohesion. In those analyses more granular material was used to fill the crater in stages 6 and 7. .

7 CONCLUSIONS

Simulating the complete dynamic soil exchange experiment has proven to be difficult. Even though the simulation was relatively simple in terms of constitutive modelling, the Modified Cam Clay model had to be amended in order to increase its robustness. Nonetheless, much improvement seems to be possible, both in terms of the numerical method used, i.e. the material point method, and in using more advanced constitutive models.

As one can see, the material points close to the axis of symmetry are very compressed and unevenly distributed. This suggests that some sort of material point merging and splitting may

be beneficial. Also, using more advanced interpolations like those described in [8-10] would help to avoid material separation. Unfortunately, these advanced techniques would increase the complexity and instability of the calculations.

The constitutive models used are rather basic. For more accurate simulations, it is essential to model rate dependency effects. The assumption of isotropy is also questionable, and may not be sufficient for the simulation.

Finally, only those calculations which successfully modelled all stages of the experiment have been shown. As such, some simulations which are more accurate during the initial stages have been discarded, typically because the final (seventh) stage of experiment could not be modelled due to numerical issues.

ACKNOWLEDGEMENTS

This research was supported by the ARC Centre of Excellence for Geotechnical Science and Engineering, headquartered at the University of Newcastle, Australia. The computations were partially undertaken using the NCI National Facility in Canberra, Australia, which is supported by the Australian Commonwealth Government. Those computational resources were provided by Intersect Australia Ltd.

REFERENCES

[1] Brackbill, J.U. and Ruppel, H.M. FLIP: a method for adaptively zoned, particle-in-cell calculations of fluid flows in two dimensions. *Journal of Computational Physics* (1986) **65**:314-346.

[2] Sulsky, D., Chen, Z. and Schreyer, H.L. A particle method for history-dependent materials. *Computer Methods in Applied Mechanics and Engineering* (1994) **118**:176-196.

[3] Sulsky D., Zhou S.J. and Schreyer H.L. Application of a particle-in-cell method to solid mechanics. *Computer Physics Communications* (1995) **87**:236-252.

[4] Bardenhagen S.G., Branckbill J.U. and Sulsky D. The material-point method for granular materials. *Computer Methods in Applied Mechanics and Engineering* 2000 **187**:529-541.

[5] Chen Z., Hu W., Shen L., Xin X. and Brannon R. An evaluation of the MPM for simulating dynamic failure with damage diffusion. *Engineering Fracture Mechanics* (2002) **69**:1873-1890.

[6] Love E. and Sulsky D.L. An energy-consistent material-point method for dynamic finite deformation placticity. *International Journal for Numerical Methods in Engineering* (2006) **57**:1323-1338.

[7] Bardenhagen S.G. and Kober E.M. The Generalized Interpolation Material Point Method. *Computer Modeling in Engineering & Sciences* (2004) **5**(6):477-495.

[8] Ma J., Lu H. and Komanduri R. Structured mesh refinement in generalized interpolation material point method (GIMP) for simulation of dynamic problems. *Computer Modeling in Engineering and Sciences* 2006 **12**:213–227.

[9] Sadeghirad A., Brannon R.M. and Burghard J. A convected particle domain interpolation technique to extend applicability of the material point method for problems involving massive deformations, *Int. J. Num. Meth. Engn* 2011 **86**:1435-1456.

[10] Sadeghirad A., Brannon R.M. and Guilkey J. Enriched convected particle domain

interpolation (CPDI) method for analyzing weak discontinuities. *Proceedings of the Particles 2011 Conference, Onate & Owen Eds.* 2011.

[11] Kanty P. and Sękowski J. Model tests of phenomena occurring during stone column formation. *Architecture Civil Engineering Environment – ACEE* (2011) **1**:45-53.

[12] Clausen J., Damkilde L. and Andersen L. Efficient return algorithms for associated plasticity with multiple yield planes. *Int. J. Numer. Meth. Engng* 2006 **66**:1036–1059.

[13] Clausen J., Damkilde L. and Andersen L. An efficient return algorithm for non-associated plasticity. *Computers and Structures* (2007) **85:**1795–1807.

[14] Alonso E.E., Gens A., Josa A. A constitutive model for partially saturated soils. *Géotechnique* (1990) **40**(3):405- 430.

[15] Sołowski W.T., Gallipoli D. Explicit stress integration with error control for the Barcelona Basic Model. Part I: Algorithms formulation. *Computers & Geotechnics.*(2010) **37**(1-2):59-67. doi:10.1016/j.compgeo.2009.07.004.